

Study of the Rabi splitting at the $5P_{3/2} \rightarrow 5D_{5/2,3/2}$ transitions in the ^{87}Rb atom upon cascade excitation in a magneto-optical trap

A.V. Akimov, E.O. Tereshchenko, S.A. Snigirev,
A.Yu. Samokotin, A.V. Sokolov, V.N. Sorokin

Abstract. The level splitting appearing upon cascade excitation of the $5D_{5/2}$ and $5D_{3/2}$ levels of the ^{87}Rb atom in a magneto-optical trap is studied experimentally. The $5S_{5/2}$ and $5P_{3/2}$ levels are coupled by a cooling laser field, the Rabi frequency being comparable with the rate of spontaneous decay of the $5P_{3/2}$ level. The experimental spectral profiles are compared with a theoretical model.

Keywords: laser cooling of atoms, Rabi frequency, Rabi splitting, magneto-optical trap.

1. Introduction

The laser cooling of atoms provides spectroscopic studies in the absence of the noticeable influence of the Doppler effect and the time-of-flight and collision broadenings. Such unique conditions allow very precise spectroscopic measurements and measurements of weak effects to be performed [1]. In particular, it is possible to measure the Stark shift of the $5D_{5/2,3/2}$ levels for an ensemble of cold atoms [2, 3]. The population of these levels requires, however, either two-photon or cascade excitation. By using cascade excitation, it is necessary to take into account the splitting of a luminescence line of the excited atom caused by its strong interaction with the field, the so-called Rabi splitting, which can distort the measurements of level shifts [4]. Such a splitting is of interest on its own and has been studied in various experimental systems such as atoms in resonators [5, 6], quantum dots [7, 8], quantum wells, microspheres [9], and ensembles of cold atoms [10, 11].

The Rabi splitting in magneto-optical traps (MOTs) is studied most often upon excitation of Rydberg levels [11–14]. In this case, the cascade population of levels is used, as a rule, and it is desirable to have the high population of an intermediate level of the cascade. The use of the intense field at the first transition of the cascade leads to the splitting of the upper level of the corresponding transition.

For example, in [11], the excitation of the $44D$ level of the ^{87}Rb atom was considered, while in [12], the levels with the principal quantum numbers $n = 40, 41, \dots$ were excited. In practice, such a splitting permits the population of certain Rydberg states with the help of a field frequency detuned from the resonance, which is important in quantum-information problems, because the nonresonance field does not perturb atoms that are already in the Rydberg state [14]. Another important case is the splitting of levels for a single cold atom or an ensemble of cold atoms in the resonator [5, 6, 15, 16]. In this case, a high-power field is absent and the level splitting occurs due to a strong interaction of atoms with the resonator. The use of the Rabi splitting in such systems allows one, for example, to control coherently the transmission of resonance radiation, to excite strictly certain states of matter, etc. [16, 17].

In the case of cascade excitation with the use of the high-power laser radiation at the first stage, the splitting of energy levels in the resonance approximation of a two-level system interacting with the light field appears when the condition $\Omega^2 + \delta^2 > (\gamma_e - \gamma_g)^2$ is fulfilled and is determined by the expression $\Omega_{\text{tot}} = [\Omega^2 + \delta^2 - (\gamma_e - \gamma_g)^2]^{1/2}$ [18], where Ω is the Rabi frequency; δ is the frequency detuning of the light field from the exact resonance with the transition frequency; and γ_e and γ_g are the decay probabilities of the upper and lower levels, respectively. In many cases, the Rabi splitting is measured by neglecting the contribution of the spontaneous decay. For example, the Rabi splitting was considered in [11, 12] for the ratios $\Omega/\gamma_e \sim 5-10$ and the contribution of the term $(\gamma_e - \gamma_g)$ was neglected. This contribution becomes, however, rather significant in a MOT where the MOT cooling radiation is used as the first excitation stage. In this case, the Rabi frequency is close to the transition width and the contribution of the term $(\gamma_e - \gamma_g)$ can be considerable.

During the interaction of a strong monochromatic field with a two-level system (Fig. 1b), the splitting of levels does not cause the splitting of lines [19] because transitions appear only between the pairs of levels with the same difference of energies. Nevertheless, the Rabi splitting can be experimentally observed in a three-level system, when the splitting is produced by a high-power laser radiation at the frequency of one transition (for example, the $5S_{1/2} \rightarrow 5P_{3/2}$ transition in Fig. 1b), while the probe laser radiation interacts with the system at another transition (for example, the $5P_{3/2} \rightarrow 5D_{5/2}$ transition in Fig. 1b). Thus, although the splitting can be obtained by using the two-level model, the calculation of the resonance profile requires the use of the three-level model [20, 21]. In practice, most of atomic systems, in which the Rabi splitting is observed, contain much more than three

A.V. Akimov, E.O. Tereshchenko, S.A. Snigirev, A.Yu. Samokotin,
A.V. Sokolov, V.N. Sorokin P.N. Lebedev Physics Institute, Russian
Academy of Sciences, Leninsky prosp. 53, 119991 Moscow, Russia;
Moscow Institute of Physics and Technology (State University),
Institutskii per. 9, 141700 Dolgoprudnyi, Moscow region, Russia;
e-mail: alakimov@lebedev.ru

Received 9 September 2009; revision received 3 November 2009
Kvantovaya Elektronika 40 (2) 139–143 (2010)
Translated by M.N. Sapozhnikov

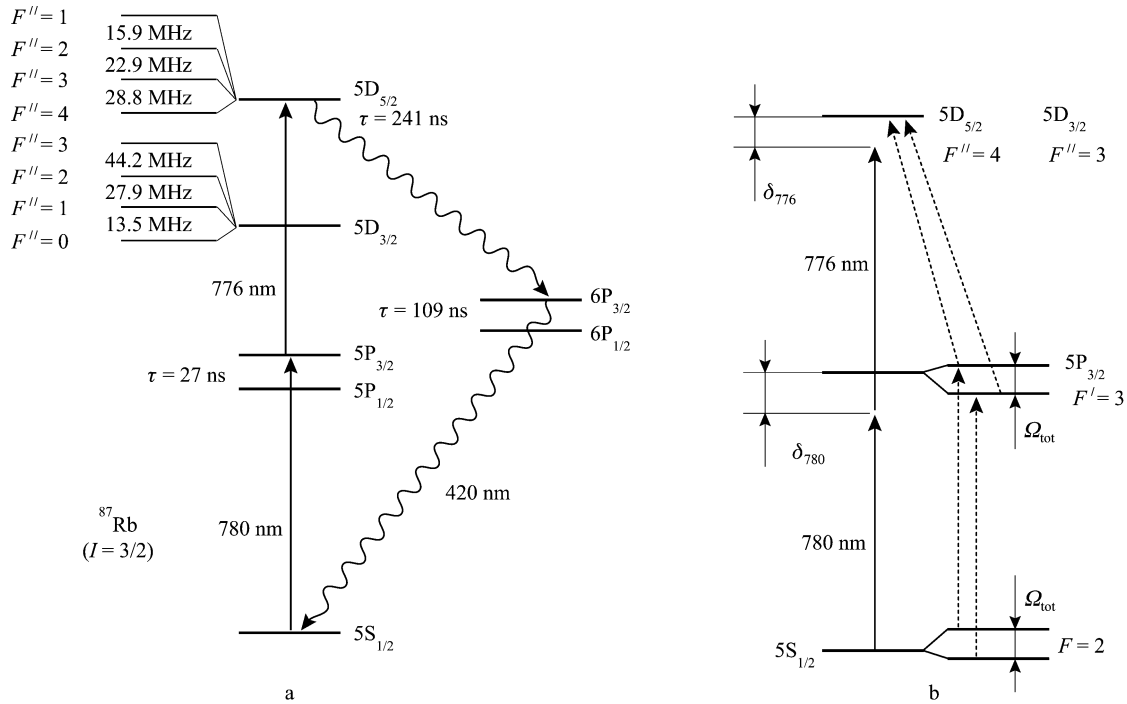


Figure 1. Energy level diagram of the ^{87}Rb atom [26, 27] considered in the present paper (a) and level splittings due to interaction with the 780-nm laser radiation and notation of laser detunings used in the text (b). The dashed arrows in Fig. 1b show the allowed transitions ($\tau = 1/\gamma$ is the level lifetime).

levels. However, it was shown in a number of experimental papers that the description of the resonance shape based on the simplest three-level model was quite acceptable [11, 13]. At the same time, some authors point out to the necessity of more careful calculations taking into account the details of the experiment and atomic structure [4, 22, 23].

In this paper, we studied experimentally the Rabi splitting upon cascade excitation of the $5D_{5/2}$ and $5D_{3/2}$ levels in a continuously running MOT. The experimental shapes of the lines were compared with the line shapes calculated by using the three-level model [21] to verify the applicability of this model for analysing the results of planned measurements of the Stark level shifts.

2. Experimental

The central part of our setup (Fig. 2) is a MOT, which was described in detail in [24]. The laser system of the MOT consists of three lasers: the master laser, the slave laser, and the transfer laser. The master and transfer lasers (the SDL7140-201 model, Sanyo) are equipped with external resonators assembled in the Littrow orientation to tune to resonance transitions in the ^{87}Rb atom at ~ 780 nm. The wavelengths of the lasers were stabilised by means of saturated absorption signals with frequency-modulation spectroscopy at the counterpropagating beam configuration in an atomic vapour cell. The radiation frequency of the master laser is stabilised with the help of a feedback loop with respect to the frequency of one of the strong cross resonances with a detuning controlled by an acousto-optic modulator (AOM). The laser radiation frequency is detuned by 5–20 MHz to the red from the frequency of the cyclic cooling $5S_{1/2} (F=2) \rightarrow 5P_{3/2} (F'=3)$ transition. The master laser radiation is amplified by the slave laser (the GH0781JA2C model, Sharp). The radiation is filtered spatially in a single-mode fibre and coupled to the trap

through this fibre. The transverse radiation intensity distribution measured at the fibre output is Gaussian. The laser beam power is ~ 12 mW. The laser beam is expanded (its radius at the $1/e$ intensity level increases up to 2.5 mm) and is divided into six MOT beams. The radiation frequency of the transfer laser is tuned to the $5S_{1/2} (F=1) \rightarrow 5P_{3/2} (F'=2)$ transition frequency similarly. The transfer laser beam is made coincident with the cooling radiation beam. The transfer laser radiation power entering the trap is ~ 2 mW.

The $5P_{3/2}$ level in the operating trap (Fig. 1a) is populated by the cooling radiation, and therefore atoms were excited to the $5D_{5/2}$ level by a cw external-cavity diode laser

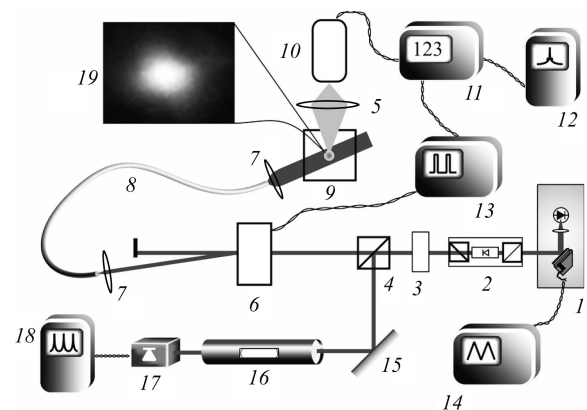


Figure 2. Scheme of the experimental setup: (1) 776-nm laser; (2) optical isolator; (3) half-wave phase plate; (4) polarisation beamsplitter cube; (5) lens; (6) AOM; (7) aspherical lens; (8) optical fibre; (9) vacuum volume of the MOT; (10) PMT; (11) photon counter; (12, 18) digital oscilloscopes; (13) pulse generator; (14) multifunctional generator; (15) mirror; (16) optical spectrum analyser; (17) photodiode; (19) photograph of a cloud of cold atoms.

(probe laser) emitting at a wavelength of 776 nm corresponding to the $5P_{3/2} \rightarrow 5D_{5/2}$ transition. The radiation of this laser was delivered to cooled atoms with the help of an optical fibre with a collimator so that its propagation direction made nonzero angles with all laser beams of the MOT. The population of the $5D_{5/2}$ level can be conveniently measured by the intensity of radiation emitted from the $6P_{3/2}$ level (its population is proportional to the $6D_{5/2}$ level population) at 420 nm (Fig. 1a). This radiation was detected with a Hamamatsu R1925 photomultiplier operating in the photon-counting regime. A blue optical filter mounted in front of the photomultiplier attenuated radiation in the region from 750 to 800 nm by more than five orders of magnitude. In this case, resonance fluorescence and scattering of laser radiation in the MOT made no contributions to photon counting.

One of the specific features of spectroscopic studies in the operating trap is a strong influence of the radiation of probe lasers on the number of atoms in the trap, which complicates the measurements of level populations [24]. To avoid this influence, we performed pulsed measurements, not switching on the probe radiation for most of the time. For this purpose, we used an AOM to which 100- μ s voltage pulses with a period of 2 ms were fed. The output pulses of the photomultiplier were counted with an SR-400 counter (Stanford Research Systems, Inc.) synchronously with pulses fed to the AOM. Spectral lines were scanned for ~ 1 s, which allowed us to observe visually the influence of the 776-nm radiation on the total number of atoms in the trap by changing the intensity of luminescence from the $5P_{3/2}$ level and selecting the optimal off-duty ratio of the signal.

3. Results and discussion

The typical output signal of the counter observed upon excitation of the $5D_{5/2}$ level is shown in Fig. 3a. One can see that the spectrum exhibits at least four spectral lines. Based on the measured frequency splittings, lines 2, 3, and 4 can be assigned to resonances corresponding to the $5P_{3/2} (F' = 3) \rightarrow 5D_{5/2} (F'' = 4, 3, 2)$ transitions, while line 1 corresponds to the side resonance of the Rabi splitting. The first group of the lines satisfies the two-photon resonance condition, while the side resonance satisfies the condition of cascade nonresonance population of the $F'' = 4$ level [21]. The Rabi splitting is even more pronounced upon excitation of the $5D_{3/2}$ level (Fig. 4a). The splitting of the hyperfine structure sublevels of this level exceeds almost twice this splitting for the $5D_{5/2}$ level [25]. In this case, the lines corresponding to the Rabi splitting prove to be completely isolated and are observed for both allowed transitions $5P_{3/2} (F' = 3) \rightarrow 5D_{5/2} (F'' = 3)$ and $5P_{3/2} (F' = 3) \rightarrow 5D_{3/2} (F'' = 2)$. It is important to point out that the energy of the hyperfine structure levels of the $5D_{5/2}$ level decreases with increasing F'' and this energy for the $5D_{3/2}$ level increases, whereas the position of the low-intensity Rabi splitting resonance depends on the absolute laser detuning. Thus, the side resonance is always located at lower frequencies with respect to the frequency of transitions corresponding to two-photon resonances, which indeed was observed in experiments.

The dependences of the ($5D_{3/2}$ or $5D_{5/2}$) upper-level population on the detuning δ_{776} at 776 nm, obtained by the convolution of the solution of system (3.11) from

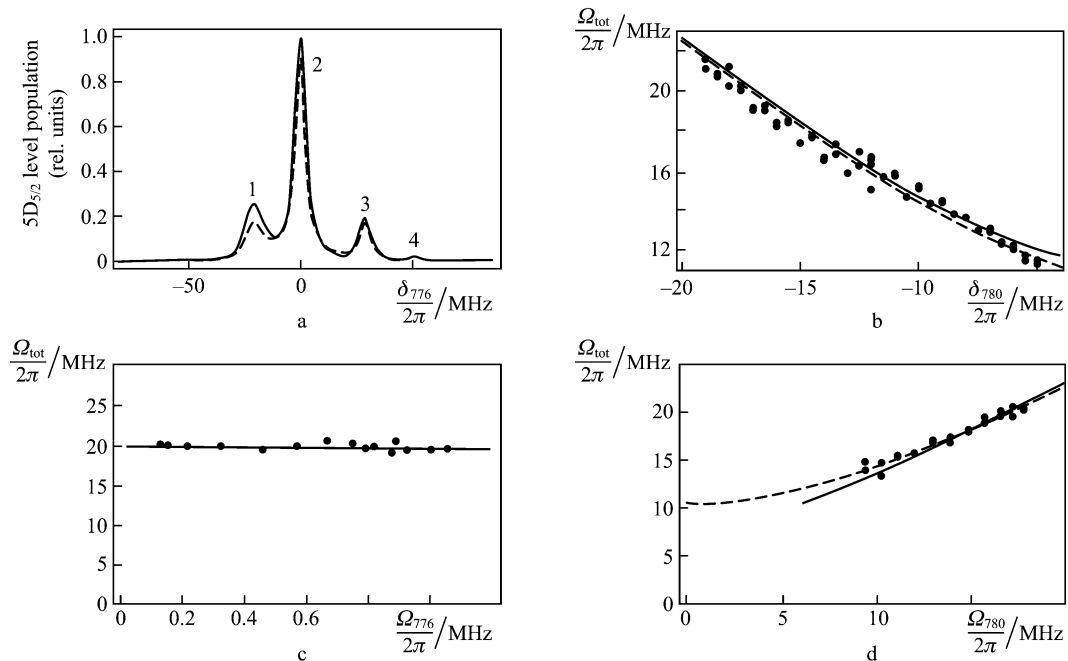


Figure 3. Dependences of the $5D_{5/2}$ level population on the detuning δ_{776} (the solid curve is experiment, the dashed curve is calculated by using model [21] for $\delta_{780}/2\pi = -12$ MHz, $\Omega_{776}/2\pi = 1$ MHz, and $\Omega_{780}/2\pi = 17$ MHz) (a); dependences of the Rabi splitting on the detuning δ_{780} (points are experiment, the solid curve is calculated by using model [21] for $\Omega_{780}/2\pi = 17$ MHz and $\Omega_{776}/2\pi = 1$ MHz, the dashed curve is calculated by expression (1) for $\Omega_{780}/2\pi = 17$ MHz) (b); dependences of the Rabi splitting on the Rabi frequency Ω_{776} for the probe laser (points are experiment, the solid curve is calculated by using model [21] for $\Omega_{780}/2\pi = 17$ MHz and $\delta_{780}/2\pi = -12$ MHz) (c); dependences of the Rabi splitting on the Rabi frequency Ω_{780} for the cooling laser [points are experiment, the solid curve is calculated by using model [21] for $\Omega_{776}/2\pi = 1$ MHz and $\delta_{780}/2\pi = -12$ MHz, the dashed curve is calculated by expression (1)] (d). The zero detuning of the radiation frequency of the 776-nm laser corresponds to the exact two-photon resonance with the $5S_{1/2} (F = 2) \rightarrow 5P_{3/2} (F = 3) \rightarrow 5D_{5/2} (F = 4)$ transition frequency.

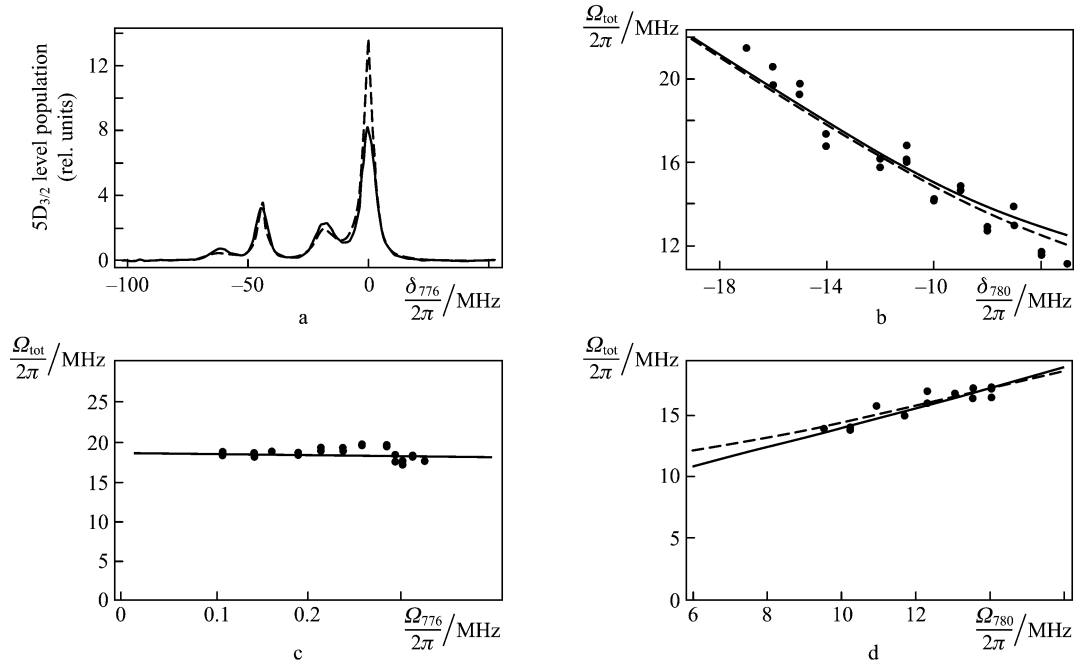


Figure 4. Dependences of the $5D_{3/2}$ level population on the detuning δ_{776} (the solid curve is experiment, the dashed curve is calculated by using model [21] for $\delta_{780}/2\pi = -12$ MHz, $\Omega_{776}/2\pi = 0.3$ MHz, and $\Omega_{780}/2\pi = 15.2$ MHz) (a); dependences of the Rabi splitting on the detuning δ_{780} [points are experiment, the solid curve is calculated by using model [21] for $\Omega_{780}/2\pi = 13.4$ MHz and $\Omega_{776}/2\pi = 0.3$ MHz, the dashed curve is calculated by expression (1)] (b); dependences of the Rabi splitting on the Rabi frequency Ω_{776} for the probe laser (points are experiment, the solid curve is calculated by using model [21] for $\Omega_{780}/2\pi = 15.2$ MHz and $\delta_{780}/2\pi = -12$ MHz) (c); dependences of the Rabi splitting on the Rabi frequency Ω_{780} for the cooling laser [points are experiment, the solid curve is calculated by using model [21] for $\Omega_{776}/2\pi = 0.3$ MHz and $\delta_{780}/2\pi = -12$ MHz, the dashed curve is calculated by expression (1)] (d). The zero detuning of the radiation frequency of the 776-nm laser corresponds to the exact two-photon resonance with the $5S_{1/2} (F=2) \rightarrow 5P_{3/2} (F=3) \rightarrow 5D_{3/2} (F=3)$ transition frequency.

[21]* with a Lorentzian with the FWHM of 1.5 MHz, which takes into account the laser linewidth, are presented in Figs 3a and 4a. One can see that by and large the model well describes the observed spectra; however, the intensity of the lines differs from the calculated intensity, especially for the $5D_{3/2}$ level. Such a difference, which was also pointed out in [11], can be explained by the fact that the system under study considerably differs from the three-level system and also by the specific features of the experiment geometry and polarisation of light, which were neglected in [21].

Figures 3b and 4b present the dependences of the Rabi splitting of the cascade $5S_{1/2} (F=2) \rightarrow 5P_{3/2} (F'=3) \rightarrow 5D_{5/2} (F''=4)$ transition on the cooling laser frequency detuning δ_{780} . The splitting was measured by approximating experimental curves by four Lorentzian curves. As expected, distances between the lines corresponding to the hyperfine structure remained constant in all experiments, while the line corresponding to the side resonance of the Rabi splitting shifted. The Rabi splitting was calibrated by the known hyperfine splitting of the upper level. The Rabi splittings found in this way are well described both by the expression

$$\Omega_{tot} = \sqrt{\Omega_{780}^2 + \delta_{780}^2 - (\gamma_{5D} - \gamma_{5P})^2} \quad (1)$$

(where γ_{5D} and γ_{5P} are the decay probabilities of the $5D$ and $5P$ levels, respectively) and the dependence obtained by using the three-level model [21] (Figs 3c, d and 4c, d). In the latter case, the calculation was performed by determining the

dependence of the upper-level population on the detuning δ_{776} (Fig. 1b) and then approximating the obtained curve by a sum of two Lorentzian curves, the distance between them being treated as the Rabi splitting.

By and large based on the experimental dependences, we can conclude that the model proposed in [21] adequately describes the Rabi splitting, although it does not predict correctly the line intensities. The strong dependence of the position of the line corresponding to the side resonance on the cooling radiation parameters and the known calculated shape of the resonance curve (taking into account the measured corrections for the amplitude) will allow us to exclude completely the contribution of the Rabi splitting in the planned measurements of the Stark shift of optical resonances.

4. Conclusions

We have studied experimentally the Rabi splitting of spectral lines corresponding to the $5S_{1/2} \rightarrow 5P_{3/2} \rightarrow 5D_{5/2}$ and $5S_{1/2} \rightarrow 5P_{3/2} \rightarrow 5D_{3/2}$ in the ^{87}Rb atom. The dependences of the splittings of the Rabi frequencies have been considered for each of the light fields and on the frequency detuning of the cooling laser from the atomic $5S_{1/2} \rightarrow 5P_{3/2}$ transition frequency. It has been shown that the obtained profiles of resonance curves are satisfactorily described by the three-level model of an atom interacting with two light fields. The model correctly describes the splitting of resonances, while their calculated amplitudes differ somewhat from experimental values.

* Note that it seems that expressions presented in appendix in [21] contain a misprint because calculations based on them lead to complex populations.

Acknowledgements. This work was supported by the Russian Foundation for Basic Research (Grant Nos 08-07-00127-a and 09-02-00649-a), the Foundation for Assistance of the Native Science, and programs of the Presidium of the Russian Academy of Sciences and the Department of Physical Sciences of the Russian Academy of Sciences.

References

1. Metcalf H.J., van der Straten P. *Laser Cooling and Trapping* (New York: Springer, 1999).
2. Kondrat'ev D.A., Beigmn I.L., Vainshtein L.A. *Kratk. Soobshch. Fiz.*, **35** (12), 3 (2008).
3. Kamenski A.A., Ovsianikov V.D. *J. Phys. B: At. Mol. Opt. Phys.*, **39**, 2247 (2006).
4. Picque J.L., Pinard J. *J. Phys. B: At. Mol. Phys.*, **9** (5), L77 (1976).
5. Carmichael H.J., Brecha R.J., Raizen M.G., Kimble H.J., Rice P.R. *Phys. Rev. A*, **40** (10), 5516 (1989).
6. Zhu Y., Gauthier D.J., Morin S.E., Wu Q., Carmichael H.J., Mossberg T.W. *Phys. Rev. Lett.*, **64** (21), 2499 (1990).
7. Kroner M., Lux A.C., Seidl S., Holleitner A.W., Karrai K., Badolato A., Petroff P.M., Warburton R.J. *Appl. Phys. Lett.*, **92**, 031108 (2008).
8. Pawlis A., Khartchenko A., Husberg O., As D.J., Lischka K., Schikora D. *Solid State Commun.*, **123**, 235 (2002).
9. Hiroshi Ajiki, Toshikazu Kaneno, Hajime Ishihara. *Phys. Rev. B*, **73**, 155322 (2006).
10. Sheludko D.V., Bell S.C., Vredembregt E.J.D., Scholten R.E. *J. Phys.: Conf. Ser.*, **80**, 012040 (2007).
11. Teo B.K., Feldbaum D., Cubel T., Guest J.R., Berman P.R., Raithel G. *Phys. Rev. A*, **68**, 053407 (2003).
12. Grabowski A., Heidemann R., Löw R., Stuhler J., Pfau T. *Fortschritte der Physik*, **54** (8-10), 765 (2006).
13. Ates C., Pohl T., Pattard T., Rost J.M. *Phys. Rev. Lett.*, **98**, 023002 (2007).
14. Deiglmayr J., Reetz-Lamour M., Amthor T., Westermann S., de Oliveira A.L., Weidemüller M. *Opt. Commun.*, **264**, 293 (2006).
15. Boca A., Miller R., Birnbaum K.M., Boozer A.D., McKeever J., Kimble H.J. *Phys. Rev. Lett.*, **93**, 233603 (2004).
16. Jiepeng Zhang, Gessler Hernandez, Yifu Zhu. *Opt. Express*, **16** (11), 7860 (2008).
17. Walls D.F., Milburn G.J. *Quantum Optics* (Berlin–Heidelberg: Springer-Verlag, 2008).
18. Shalagin A.M. *Osnovy nelineinoi spektroskopii vysokogo razresheniya. Uchebnoe posobie* (Fundamentals of High-resolution Nonlinear Spectroscopy. Educational Manual) (Novosibirsk, Novosibirsk State University, 2008).
19. Delone N.B., Kraiov V.P. *Usp. Fiz. Nauk*, **124**, 619 (1978).
20. Berman P.R., Salomaa R. *Phys. Rev. A*, **25**, 2667 (1982).
21. Whitley R.M., Stroud C.R. Jr. *Phys. Rev. A*, **14** (4), 1498 (1976).
22. Fisk P.T.H., Bachor H.-A., Sandeman R.J. *Phys. Rev. A*, **33** (4), 2418 (1986).
23. McClean W.A., Swain S. *J. Phys. B: At. Mol. Phys.*, **10** (5), 1673 (1977).
24. Akimov A.V., Tereshchenko E.O., Snigirev S.A., Samokotin A.Yu., Sokolov A.V., Kolachevskii N.N., Sorokin V.N. *Zh. Eksp. Teor. Fiz.*, **136**, 419 (2009).
25. Marian A., Stowe M.C., Lawall J.R., Felinto D., Ye J. *Science*, **306**, 2063 (2004).
26. Ralchenko Yu., Kramida A.E., Reader J. *National Institute of Standard and Technology. Atomic Spectra Database (version 3.1.4)*; <http://physics.nist.gov/asd3>.
27. Smith P.L., Heise C., Esmond J.R., Kurucz R.L. *Atomic Spectral Line Database*; <http://www.pmp.uni-hannover.de/cgi-bin/ssi/test/kurucz/sekur.html>.